



Cite this: *RSC Adv.*, 2024, **14**, 8090

## Study of ternary deep eutectic solvents to enhance the bending properties of ash wood

Ruocai Bai, <sup>ab</sup> Wenhao Wang, <sup>ab</sup> Mengyao Chen<sup>ab</sup> and Yan Wu <sup>ab</sup>

Deep eutectic solvents (DESs) are considered one of the most promising biomass pretreatment reagents, and their research applications in woody fibrous biomass are increasing yearly. Inspired by the research related to wood bending, we explored the effects of different DES systems on the bending development of wood, and the results showed that the addition of anhydrous ferric trichloride to the DES system of lactic acid/choline chloride could enhance the treatment effect that increased the bendability and torsion resistance of ash wood. The anhydrous  $\text{FeCl}_3$  could act as an active site and provide acidic protons to improve the treatment efficiency of DES. In addition, the addition of an appropriate amount of water can reduce the viscosity of the DES system, and the highest lignin removal rate was obtained at 10 wt% of water in the DES, which resulted in the best mechanical properties and tensile resilience of ash wood, with the tensile strength and stability of 97 MPa and 13.6%, respectively, as determined by experiments with different water contents in different mass fractions. Therefore, using a DES can effectively improve the bending properties of wood.

Received 14th January 2024

Accepted 1st March 2024

DOI: 10.1039/d4ra00357h

rsc.li/rsc-advances

### 1. Introduction

Wood is a versatile natural material that can be used in a wide range of applications. Ash wood is a widely used hardwood tree known for its uniform texture and apparent grain. It is commonly used in producing carvings, musical instruments, furniture, and architectural decoration due to its adaptability and attractive appearance.<sup>1</sup> But, the compressive and tensile strengths of ash wood are low.<sup>2</sup> However, due to its physical and mechanical properties, it sometimes requires a softening treatment. The multiple reactions of deep eutectic solvent (DES) with ash wood boards can improve the plasticity of wood, reduce its hardness, and make it easier to process, broadening their scope of use,<sup>3</sup> help upgrade traditional wood products to green functional wood products, and provide a new wood modification method.<sup>4</sup>

At present, there are various methods to achieve wood bending, including hydrothermal, high-frequency current, microwave heating, and chemical treatment.<sup>2</sup> Mubarok *et al.*<sup>5</sup> have carried out wood modification experiments using chemical treatment and have improved the performance of beech. M. L. de Peres *et al.*<sup>6</sup> have explored the change of bending properties of wood at different temperatures and humidity through controlled experiments. However, traditional chemical treatments for wood may destroy the natural cellulose crystal

structure of wood,<sup>7</sup> leading to rupture and collapse of the wood cell wall and ultimately damaging the structure of the wood and reducing its physical and mechanical properties.<sup>8</sup> In addition, these commonly used chemical agents are often relatively toxic, corrosive and difficult to recycle, which can cause a lot of pollution and have a negative impact on the environment.

A deep eutectic solvent is a mixture of a hydrogen bond donor (HBD) and hydrogen bond acceptor (HBA) associated with each other through strong hydrogen bonding at a proper molar ratio, and its melting point is much lower than that of the individual components.<sup>9</sup> DESs are emerging green solvents with the advantages of low cost, low toxicity, and easy preparation.<sup>10</sup> A DES can selectively separate lignin with high purity, low molecular weight, and small dispersion coefficients, making it a promising option for separating lignocellulosic fibre components.<sup>11</sup> As more people focus on “green chemistry,” using deep eutectic solvents as a new green solvent is becoming increasingly common.<sup>12</sup>

The selective removal ability of wood hemicellulose and lignin by binary or ternary eutectic solvents composed of different components is different, which will affect the hardness, elasticity and toughness of plastic wood.<sup>13</sup> However, in the binary DES system, the efficiency of lignin removal can be improved by increasing the hydrogen bond strength of the DES by increasing the ratio of hydrogen bond donors. Therefore, it is a more effective method to remove lignin with a terene DES composed of double hydrogen bond donors and hydrogen bond receptors. Xing *et al.*<sup>14</sup> formulated a novel ternary DES with double hydrogen bond donors using choline chloride, formic acid, and acetic acid according to the molar ratio of 1:1:1 for

<sup>a</sup>College of Furnishings and Industrial Design, Nanjing Forestry University, Nanjing 210037, China. E-mail: wuyan@njfu.edu.cn

<sup>b</sup>Co-Innovation Center of Efficient Processing and Utilization of Forest Resources, Nanjing Forestry University, Nanjing 210037, China



use in the biomass pretreatment and extraction of straw. The results showed that this ternary DES system treated lignin significantly better than the same type of binary DES. Xia *et al.*<sup>15</sup> used a binary DES formulated with choline chloride and glycerol at a molar ratio of 1 : 2. They found that the strength of the hydrogen bonds in the binary DES was not high enough to break the ether bonds in lignin, and it showed a weak breaking effect on the hydrogen bonds of lignin. In this paper, a ternary DES was formulated by adding ferric chloride ( $\text{FeCl}_3$ ) to a binary DES. This enables it to simultaneously break down the hydrogen and ether bonds in lignin, making it an effective method for lignin removal.

In the preparation of multicomponent DESs, although the composition of different raw materials has a specific effect on its performance, the influence of solvent composition in the system is often ignored.<sup>16</sup> Therefore, it is essential to explore the impact of different solvent components on the performance of DESs. Among the many solvents, water is the most common and cheapest solvent. Water has a dual impact on deep eutectic solvents. On the one hand, it can decrease the viscosity of a DES and act as a hydrogen bond donor and acceptor, thereby increasing the polarity of deep eutectic solvents.<sup>17</sup> On the other hand, water can disrupt the hydrogen bonding effect and prevent the deep eutectic solvents from having their desired effect.<sup>18</sup>

In this work,  $\text{FeCl}_3$  was introduced as a new acidic proton and active site to form a ternary low eutectic solvent system with lactic acid and choline chloride. A series of multicomponent DES with different moisture content were designed and prepared. The DES has a wide range of physical and chemical properties and is applied to the multifunctional modification of ash wood. The effect of the DES on the mechanical properties of ash wood was evaluated. The specific effects of different components and different moisture content were elucidated. This work highlights the role of new DESs in the functional modification of wood.

## 2. Experimental section

### 2.1 Materials and chemicals

The materials used in this experiment were ash wood (*Fraxinus excelsior* L.) samples with dimensions of 3 mm (thickness)  $\times$  5 mm (width)  $\times$  150 mm (length), provided by Shantou Yihua Life Science and Technology Company Limited, Shantou, China. Anhydrous ethanol was sourced from Guanghua Science and Technology Co. in Guangdong Province, China, while acetone was provided by Beijing Chinese Medicine Chemical Reagent Co. Choline chloride (AR, 98%) was supplied by Shanghai Kansbeck Scientific Instrument Co. Lactic acid (AR, 85–92%) was from Tianjin Fuyu Fine Chemical Co. Anhydrous ferric chloride (AR, 97%) was purchased from Shanghai Aladdin Biochemical Technology Co. All of the chemicals used were of analytical grade.

### 2.2 Preparation of DES

The corresponding quantities of choline chloride and lactic acid were added to the beaker using a balance according to the molar

ratio 1 : 10. And 0, 10 and 20 wt% distilled water were added as variables. The liquid was stirred at 60 °C with a magnetic stirrer until it formed a colourless transparent liquid, named BES-1, BES-2 and BES-3, respectively. As a control, choline chloride with a molar ratio of 1 : 10 : 1, lactic acid, and catalyst  $\text{FeCl}_3$  were added to the reagent, and the above steps were repeated. The resulting solutions were named TES-1, TES-2, and TES-3. The specific DES design and experimental conditions are shown in Table 1.

### 2.3 Preparation of modified wood

Firstly, ash wood strips were soaked in a 1 : 1 volume ratio solution of anhydrous ethanol and acetone for 10 h to remove wood extractives such as gums and resins from the wood. Then, the wood strips were dried in an oven at 102 °C for 6 h to remove residual solvents and moisture. The pretreated ash wood strips were then added to DES and heated in a water bath at 95 °C for 6 h. The samples at the end of the treatment were then rinsed several times with deionized water to remove the reagents remaining in the wood and the stripped lignin. Finally, the samples were dried in a freeze-dryer at –60 °C for 48 h. Finally, all the samples were pre-frozen at –15 °C for 6 h and then vacuumed at –56 °C for 36 h to obtain the dried modified ash wood strips. Fig. 1 shows the demonstration of the experimental procedure.

In order to facilitate distinction, the natural ash wood is referred to as NW, while the sample treated with Binary DES is called BW (Binary DES Wood). Using BW-1 as an example, its corresponding DES reagent is BES-1, and so on to obtain BW-2 and BW-3. The sample treated with Ternary DES is referred to as TW (Ternary DES). Using TW-1 as an example, its corresponding DES reagent is TES-1, and so on to get TW-2 and TW-3.

### 2.4 Measurements and characterization

To observe the micro-morphological characteristics of the samples, a FEI Quanta 200 scanned electron microscope (SEM) was used to observe the samples at an accelerating voltage of 30 kV. The X-ray diffractometer (Ultima IV, from Rigaku Co., Ltd, Tokyo, Japan) was used to characterise the molecular structure of the sample. To analyze the functional group infrared spectra of functional groups of samples, a Fourier transform infrared spectrometer (VERTEX 80V, from Bruker Co., Ltd, Bremen, Germany) was used. The X-ray diffractometer scanned the samples at a scanning voltage of 40 kV, a scanning range of  $2\theta = 5\text{--}60^\circ$ , and a scanning speed of  $10^\circ \text{ min}^{-1}$ .<sup>19</sup>

The cellulose, hemicellulose, and lignin content of the samples were tested using the National Renewable Energy Laboratory (NREL) method. The lignin and sugar content were measured separately. Lignin was measured by two-step sulfuric acid hydrolysis, while sugar was analyzed by high-performance liquid chromatography (HPLC).<sup>20</sup> To begin, measure 0.3 g of a completely dry powder sample and place it in a glass pressure bottle. Next, add 72% concentrated sulfuric acid to the bottle one drop at a time. Shake the bottle in a water bath at 30 °C for 1 hour, using the shaker every 10 minutes to ensure full contact between the sulfuric acid and the sample. Once the reaction is



Table 1 Design and formulation of DES

Type of DES	HBD	HBA	Molar ratio (HBD/HBA)	Moisture content (wt%)	Preparation temperature (°C)
BES-1	Lactic acid	Choline chloride	10 : 1	0	60
BES-2	Lactic acid	Choline chloride	10 : 1	10	60
BES-3	Lactic acid	Choline chloride	10 : 1	20	60
TES-1	Lactic acid/iron(III) chloride	Choline chloride	10 : 1 : 1	0	60
TES-2	Lactic acid/iron(III) chloride	Choline chloride	10 : 1 : 1	10	60
TES-3	Lactic acid/iron(III) chloride	Choline chloride	10 : 1 : 1	20	60

complete, dilute the mixture with ultra-pure water to a 4% concentration. Seal the bottle and place it in the autoclave. Stop heating when the temperature reaches 121 °C. The supernatant was diluted with distilled water at a certain multiple, and 3 mL of the resulting solution was measured. The absorbance was then measured at 320 nm using an ultraviolet spectrometer. Next, 2 mL of the supernatant was mixed with 50 µL of 50 wt% sodium hydroxide solution and filtered using a 0.22 µm water filter. The contents of glucose, xylan, and arabinose were analyzed using high-performance liquid chromatography (HPLC). Filter the residue using glass and wash it continuously with distilled water until it is neutral. Then, dry the filtered residue in an oven at 100 °C for 6 hours. Weigh the poor quality before and after using a balance and calculate the acid-insoluble lignin content. Finally, use formula (1) to calculate the cellulose, hemicellulose, and lignin content.

$$\text{Content} = \frac{M_S}{M_W} \times 100\% \quad (1)$$

The hardness of the samples was measured by a Shore hardness tester, and the measurement should be repeated three times at three different points for each sample and then averaged to reduce the error. Tensile fracture and three-point bending tests were conducted using a computer-controlled electronic universal mechanical testing machine. The thermal degradation of samples from 0–800 °C was tested using a thermogravimetry and synchronous thermal analyser (TGA209F3, NETZSCH, Germany) under a nitrogen atmosphere at a heating

rate of 10 °C min<sup>-1</sup>. A color difference meter (RM200QC, from Xrite Co., Ltd) was used to measure the surface color of the samples. According to GB/T 4893.4-2013 *L × a × b × standard*, use a gloss meter (X-rite ci60) to record the glossiness of samples at 20, 60, and 85° incidence angle degree, each sample measured five times, taking the average value.

### 3. Results and discussion

#### 3.1 Morphology analysis

The micro-morphological features of NW, BW, and TW can be observed by SEM images. Fig. 2a–h show the SEM images of NW, BW, and TW at 800× magnification, respectively. In addition, although Fig. 2a and b show SEM images of natural ash wood, there are differences since they were produced in different batches, and the raw materials were taken from other parts of various trees. It is necessary to take SEM images of them separately. NW is mainly composed of tough woody fibers, ducts, and ray cells; rigid woody fiber cells with small cell lumens and thick cell walls were randomly distributed between uniform single rows of woody radials.<sup>21</sup> The NW was characterised by multiple channels and a complete cellular structure by scanning electron microscopy (SEM) (Fig. 2a and e). After DES treatment, the separation of BW and TW into the interlayer region of the composite can be observed, indicating the degradation of the wood components.

As shown in Fig. 2b–d and f–h, after treatment with binary DES and ternary DES, the basic structure of BW and TW cells was maintained, but the microscopic morphology changed. In

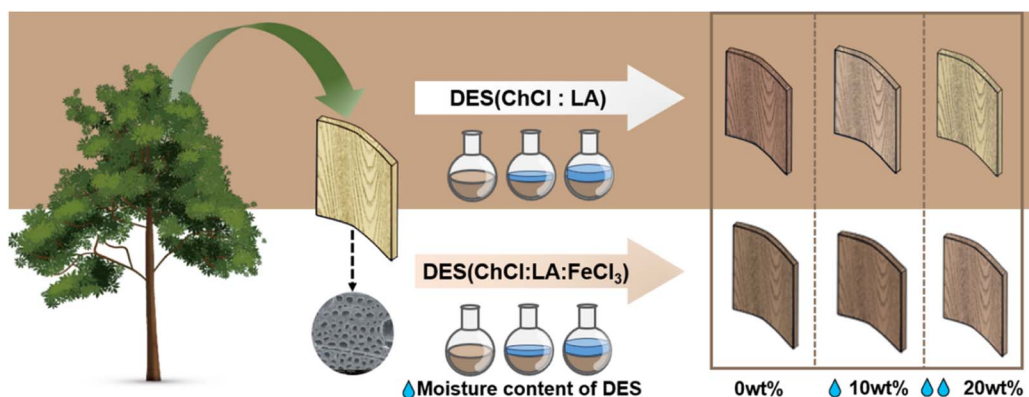


Fig. 1 Experimental process demonstration diagram.



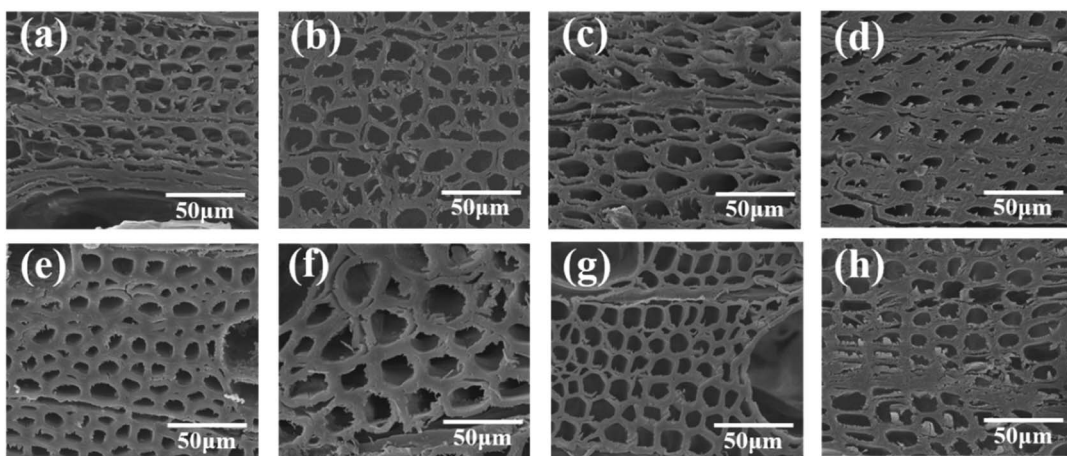


Fig. 2 SEM images of NW (a and e), BW-1 (b), BW-2 (c), BW-3 (d) and TW-1 (f), TW-2 (g), TW-3 (h) at cross-sections.

particular, cracks appeared between the cells, possibly because the lignin distributed in the intercellular layer and the corner area of the cell was selectively removed, causing the connections between the cell walls to become less tight and, thus, cracks to appear. Further comparison showed that with the change in water content in binary DES, the cell wall thinning of BW-2 was most obvious compared to BW-1 and BW-3. Compared with TW-1 and TW-3, TW-2 also showed thinning of the cell wall and enlargement of the cell cavity. Therefore, it can be concluded that whether it is binary DES or ternary DES, when the water content is 10%, the lignin removal effect of the ash wood cell wall is the best.

At the same time, it can be seen that compared to NW, the samples treated with DES, while thinning the ash cell wall, promote the connection between the cell walls and show a highly reticulated porous structure (Fig. 2c and g). This structure allows the modified ash to maintain the cell structure without collapsing under the stress of large deformation and improves the elasticity and flexibility of the ash wood.

### 3.2 Chemical structure analysis

The effects of binary and ternary DES treatments on the chemical structure of ash wood were investigated using FT-IR. As shown in Fig. 3a and b, the characteristic absorption peaks of NW were the same as in previous studies, which included  $3385\text{ cm}^{-1}$  (O-H stretching vibration),  $2918\text{ cm}^{-1}$  (C-H stretching vibration),  $1025\text{ cm}^{-1}$  (ether bonding vibration),  $1731\text{ cm}^{-1}$  (C=O stretching vibration),  $1235\text{ cm}^{-1}$  (C-O stretching vibration),  $1460$ ,  $1509$  and  $1593\text{ cm}^{-1}$  (aromatic backbone vibrations).<sup>22</sup> The absorption peaks at  $1025$ ,  $1105$  and  $1155\text{ cm}^{-1}$  represented the cellulose absorption peaks,<sup>23</sup> while the absorption peaks at  $1235\text{ cm}^{-1}$  and  $1731\text{ cm}^{-1}$  represented the hemicellulose absorption peaks.<sup>24</sup> The absorption peaks at  $1460\text{ cm}^{-1}$ ,  $1509\text{ cm}^{-1}$ , and  $1593\text{ cm}^{-1}$  represented the lignin absorption peaks. Overall, it was found that there were no significant differences in the infrared spectra of BW, TW, and NW. The DES treatment on natural ash wood selectively removed part of the lignin and hemicellulose, thereby

decreasing the intensity of the absorption peaks. The intensity of the absorption peak at lignin was reduced significantly for BW (Fig. 3a), and the decrease in intensity of the absorption peaks at  $1731\text{ cm}^{-1}$  for BW-1 and BW-2 suggested that they removed more hemicellulose.<sup>25</sup> The decrease in intensity of the absorption peaks at  $1593\text{ cm}^{-1}$  was the most prominent for TW-2, indicating that compared to TW-1 and TW-2, TW-2 had a more significant effect on the absorption peaks at  $1593\text{ cm}^{-1}$  at which lignin aromatics were best removed. Finally, from the side-by-side comparison, there is no significant difference in the absorption peaks of TW over BW. This could be due to the limitations of the IR spectrograms in quantitatively analyzing the amount of lignin removal by DES. Further research is necessary to explore this in more detail. Nevertheless, based on the data presented above, we can conclude that adding 10 wt% of water to binary or ternary DES can enhance the DES system's ability to remove lignin and hemicellulose from ash wood.

XRD was used to analyse the crystallinity of the original ash strip and its modified wood to assess whether DES would affect it. As shown in Fig. 3, the XRD pattern of NW shows three diffraction peaks:  $15.6$ ,  $22.5$  and  $34.4^\circ$ , corresponding to  $(110)$ ,  $(200)$  and  $(004)$ ,<sup>26</sup> respectively. Therefore, cellulose with good crystallinity is present in NW, and it is the characteristic peak of type I cellulose.<sup>27</sup>

It is worth noting that after DES treatment, the characteristic peak strength of cellulose of BW and TW is increased, indicating that their crystallinity is improved, among which the crystallinity of BW-2 and TW-2 is the highest, which may be due to the removal of more amorphous components (such as hemicellulose and lignin) of binary and tertiary DES, resulting in a relative increase in crystallinity.<sup>28</sup>

### 3.3 Chemical composition content analysis

Fig. 4 shows the changes in cellulose, hemicellulose, and lignin of NW, BW, and TW. The solid recovery of natural ash wood treated with ternary DES is lower (58.1% to 63.2%) as compared to binary DES (65.2% to 68.2%). This suggests that ternary DES is more effective in removing the chemical components of ash



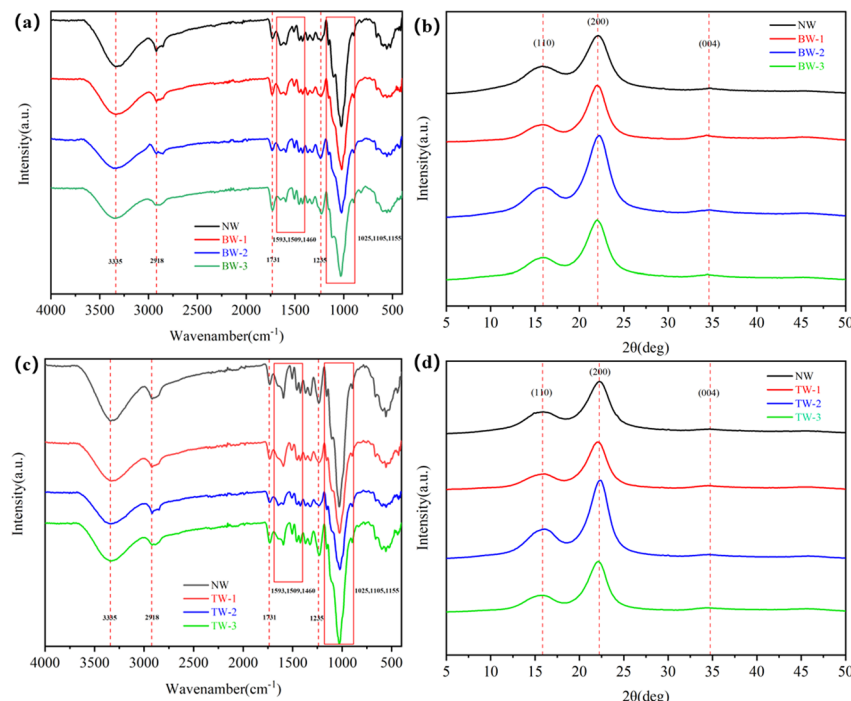


Fig. 3 FT-IR spectra of (a) NW and BW and (c) NW and TW; XRD patterns of (b) NW and BW and (d) NW and TW.

wood due to the presence of ferric chloride that provides more reactive protons and acidic sites.<sup>29</sup> As a result, ternary DES is more capable of breaking down lignin. Upon adding 10 wt% moisture to DES, the retention of wood cellulose decreased while the removal of hemicellulose and lignin increased. This suggests that the hydrogen bonding capacity increased, which facilitated the removal of hemicellulose and lignin. It is particularly noteworthy that the lignin removal rate of TW-2 in TW is the highest, which is 64.7%, and that of BW-2 in BW is the

highest, which is 48.5%, which is 16.2% higher than that of BW, indicating that ternary DES has a significant improvement in the removal effect of lignin and can effectively remove lignin in the cell wall (Table 2). The lignin content of BW and TW is much lower than NW, and the cellulose retention rate is more than 80%, which is beneficial for modified ash wood to maintain a certain mechanical strength. The removal of some lignin and hemicellulose also provides favorable conditions for improving elasticity.

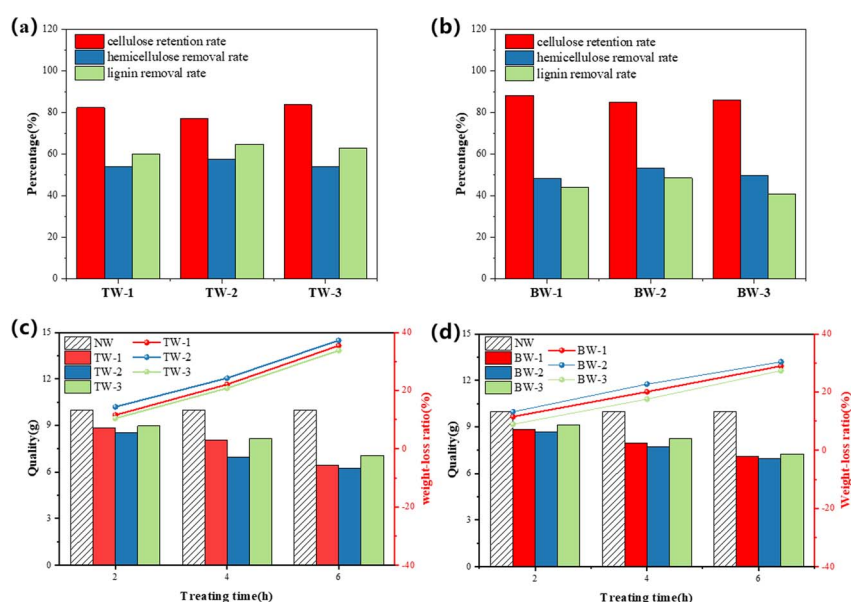


Fig. 4 Change of chemical composition of BW (a) and TW (b); weight over time of BW (c) and TW (d).



Table 2 Effects of deep eutectic solvent treatment on chemical composition of european ash<sup>a</sup>

Sample	Cellulose	Hemicellulose	Lignin	Solid recovery rate	Cellulose retention rate	Hemicellulose removal rate	Lignin removal rate
NW	46.1	17.8	26.9				
BW-1	60.4	13.5	22.4	67.8	88.2	48.6	43.8
BW-2	60.0	12.7	21.3	65.2	84.9	53.3	48.5
BW-3	62.4	13.8	23.3	68.2	86.2	49.8	40.9
NW	47.5	16.2	28.3	—	—	—	—
TW-1	62.4	11.8	18.0	62.7	82.4	54.1	60.0
TW-2	63.0	11.9	17.2	58.1	77.1	57.4	64.7
TW-3	62.9	11.8	16.6	63.2	83.8	53.9	62.9

<sup>a</sup> Unit (%).

Fig. 4c and d further shows the weight loss of BW and TW with increasing time. In this case, the bar graph represents the weight change, and the line graph represents the change in weight loss. The results showed that the effect of binary and ternary DES on ash wood intensified with increasing treatment time.

### 3.4 Mechanical performance test

Fig. 5a and b shows the tensile curves at break for NW, BW, and TW, which indicate that although the tensile strength of the modified ash wood strips decreased after binary and ternary DES treatments (1650 N to 800 N and 1700 N to 900 N),

the elongation at break increased. The reason may be that the cell walls of the modified ash wood strips became thinner, and the neighbouring cells formed stronger interactions, which compensated for the negative effect of the removal of the cell matrix.<sup>29</sup> Furthermore, the removal of some hemicellulose and lignin led to the formation of closer contact microfibrils between the cellulose. As a result, hydroxyl groups were abundant on the surface of these microfibrils, which enabled the construction of friction and hydrogen bonding between the nanofibers and microfibrils, which made the modified ash wood strips less prone to fracture.<sup>30</sup> Fig. 5c shows the elongation at the break of NW, BW, and TW.

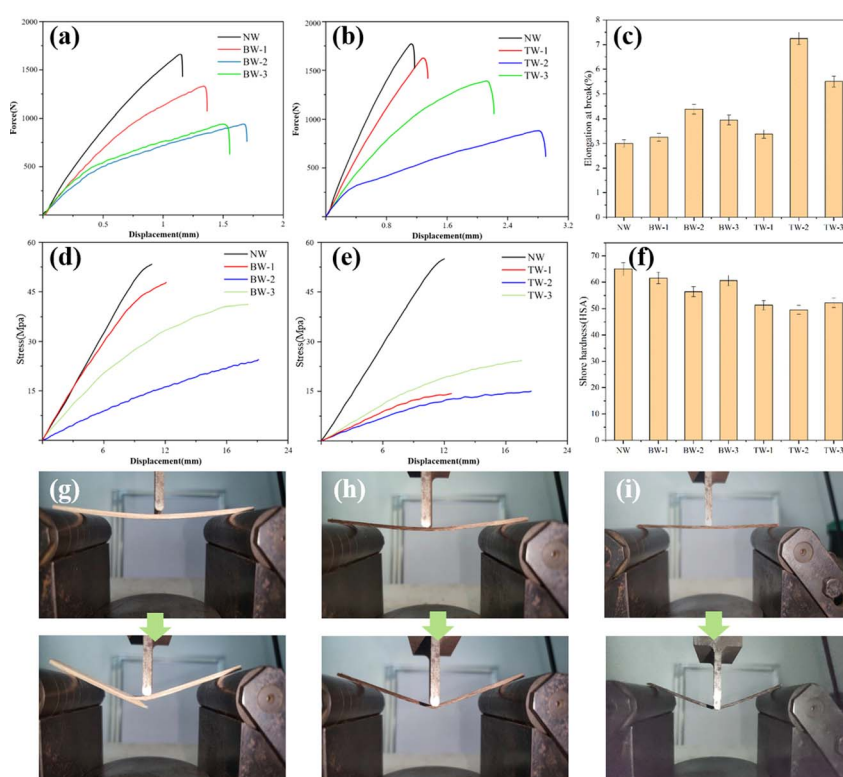


Fig. 5 Mechanical properties of NW, BW, and TW. (a) Force and displacement curves of NW and BW; (b) force and displacement curves of NW and TW; (c) elongation at break of NW, BW and TW; (d) three-point bending curves of NW and BW; (e) three-point bending curves of NW and TW; (f) Shore hardness (HSA) of NW, BW and TW; (g) three-point bending picture of NW; (h) three-point bending picture of BW-2; (i) three-point bending picture of TW-2.



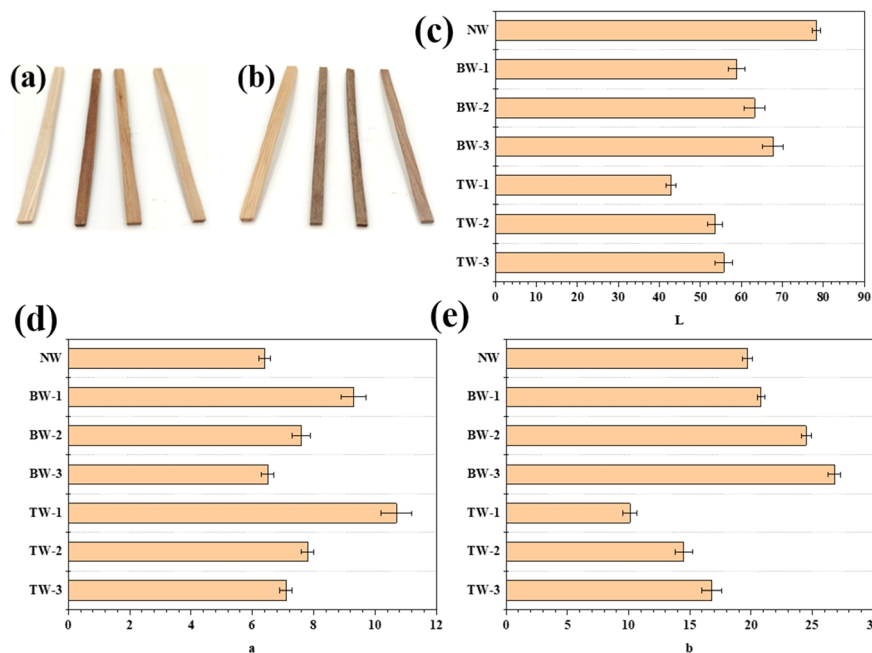


Fig. 6 NW, BW, and TW colors. (a) Samples of NW and BW; (b) samples of NW and TW; (c)  $L$  values of the NW, BW, and TW in  $L \times a \times b$  color space; (d) values of the NW, BW, and TW in  $L \times a \times b$  color space; (e)  $b$  values of the NW, BW and TW in  $L \times a \times b$  color space.

Overall, the DES-treated modified ash wood strips have a higher elongation at break than the natural ash wood strips, especially TW-2, which reaches 7.3% elongation at suspension, significantly improving compared to the 3% of NW. The reason may be that ternary DES can effectively remove both lignin and hemicellulose from the cell wall while retaining the cell structure intact (Fig. 2). At the same time, the moderate addition of water prevents the destructive effect of the high concentration of DES on the wood cells.<sup>31</sup>

Fig. 5d and e shows the three-point bending curves for NW, BW, and TW. Regarding the degree of deformation in the samples when the fracture occurred, NW was more prone to rupture during bending (displacement 10 mm). Meanwhile, BW and TW had increased flexibility and could withstand more significant deformation without fracture, and in particular, both BW-2 (displacement 19 mm) and TW-2 (displacement 20 mm) showed excellent bending performance. The DES treatment softened the ash wood cell walls, making bending easier.<sup>32</sup>

The mechanical properties of DES-treated composites can be compared with those reported in the literature. It should be noted that the initial condition of the wood and the details of the treatment method are very important, and that different directions of application also affect the mechanical properties of the material.<sup>33</sup> Ran *et al.*<sup>34</sup> treated the wood with DES, although the property was relatively stable, the Shore hardness increased from 47 to 64. Qi<sup>35</sup> used DES in an *in situ* lignin regeneration strategy to improve wood plastic composites, and the maximum fracture elongation of the sample was about 24.25% that of the log. However, the tensile strength of TW-2 increased by 2.43 times, the hardness decreased significantly, and the mechanical properties were excellent.

### 3.5 Color difference analysis

The corresponding  $L$ ,  $a$ , and  $b$  values of NW, BW, and TW in the  $L \times a \times b$  color space are shown in Fig. 6c–e. Regarding luminance  $L$ , the  $L$  values of BW and TW have decreased compared to NW (Fig. 6c). It can be seen that the values of NW, BW, and TW are positive and small, which indicates that the color of the wood of the original ash wood is reddish and that there is a slight increase in the reddish tones after treatment.  $b$  values represent the change from yellow to blue, and the  $b$  values of BW are generally slightly higher than those of NW (Fig. 6e), indicating that BW is more yellowish, and at the same time, the  $b$  values of TW are minor, meaning that BW is more yellowish. The  $b$  value represents the change from yellow to blue. The  $b$  value of BW is generally slightly higher than that of NW (Fig. 3–6e), indicating that BW is more yellow; meanwhile, the  $b$  value of TW is small, and the overall color becomes darker, which matches the results in Fig. 6b. The  $b$  value of BW is slightly higher than that of NW, indicating that BW is more yellow. The reason for this change may be that the interlinked hydrogen

Table 3 Gloss data of NW, BW, and CW

Sample	Gloss (%)		
	20°	60°	85°
NW	0.8	1.9	1.3
BW-1	0.2	1.3	1.0
BW-2	0.5	1.6	1.3
BW-3	1.6	2.2	1.9
TW-1	0.2	1.1	0.9
TW-2	0.4	1.8	1.6
TW-3	0.4	2.0	2.4



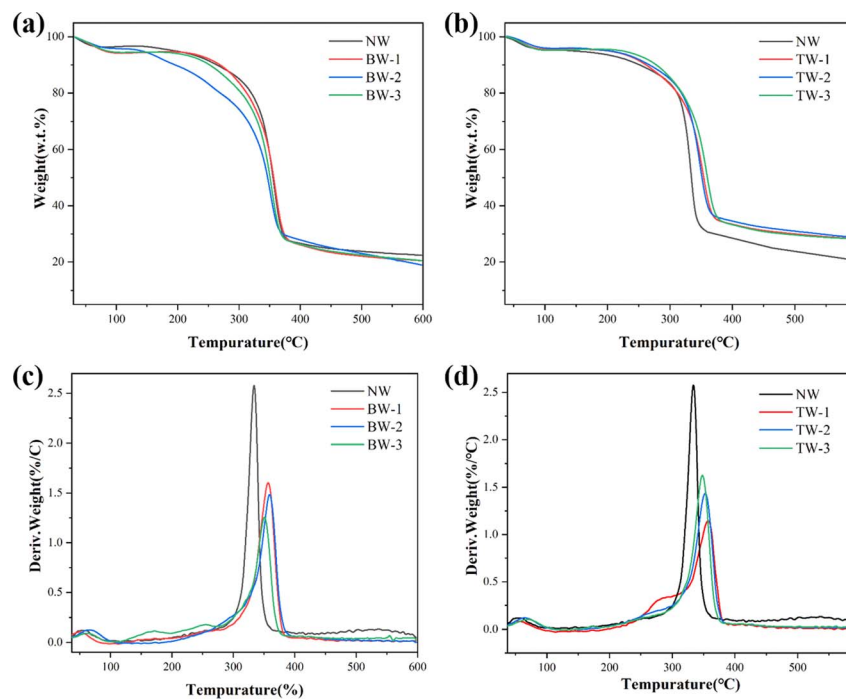


Fig. 7 (a) Typical TGA curves of NW and BW; (b) typical DTG curves of NW and BW; (c) typical TGA curves of NW and TW; (d) typical DTG curves of NW and BW.

bonds of lignin are broken during DES treatment, which in turn generates a large number of free radicals, which are unstable and efficiently react with the neighboring lignin molecular chains to form peroxides, which ultimately decompose into colored compounds and discolor the wood.<sup>35</sup>

Table 3 shows the gloss levels of NW, BW, and TW. The gloss levels of the DES-treated ash wood strips were all reduced (20, 60, 85°), consistent with the results observed in Fig. 6a and b. The reason may be that the modified ash wood strips become darker in color, absorbing more light and reducing the diffuse and specular reflections of light W, which indicate that although the tensile.

### 3.6 Thermal gravimetric analysis

The thermal stability of lignin is of great value in explaining the relationship between its intrinsic structure and chemical properties. The thermal stability properties of the samples were tested using a thermogravimetric analyzer (TG), and the typical thermogravimetric analysis (TGA) and differential thermogravimetric (DTG) curves for NW, BW, and TW are presented in Fig. 7. Lignin degradation went through three stages: initial degradation, significant degradation, and slow pyrolysis. All curves showed a slight mass loss below 100 °C, which was attributed to the evaporation of water. In the initial stage (100–180 °C), some lignin with small molecular weight began to degrade. Significant degradation occurs at 180–370 °C, where the mass of the samples decreases rapidly with increasing temperature, which is due to the cleavage of the lignin ether bond and evaporation of the monomeric phenol.<sup>36</sup> A slow degradation phase occurs at 370–600 °C, which results in the

formation of carbon due to condensation polycondensation of volatile products and demethylation of lignin.

In this experiment, the TGA curves of BW and NW were not significantly different (Fig. 7a), and only the maximum decomposition rate was reduced (Fig. 7c), indicating that the binary DES system of lactic acid/choline chloride did not have the effect of enhancing the flame retardancy of wood. However, the carbon retention rate of TW increased significantly (Fig. 7b) while the maximum decomposition rate decreased (Fig. 7d). The reason may be that the iron trichloride (FeCl<sub>3</sub>) in the ternary DES prevented the degradation of cellulose residue while increasing the pyrolysis temperature of modified ash wood.<sup>37</sup>

Table 4 shows the thermogravimetric data of NW, BW, and TW. It is found that the  $T_{\max}$  of NW is lower than that of BW and

Table 4 Thermogravimetric data of NW, BW and TW<sup>a</sup>

Sample	$T_0$ (°C)	$T_f$ (°C)	$T_{\max}$ (°C)	Residue at 600 °C (%)
NW	249.5	375.9	333.6	22.4
BW-1	245.2	379.5	356.5	20.5
BW-2	248.4	367.1	359.2	18.9
BW-3	250.7	373.3	350.8	20.4
TW-1	242.1	375.1	358.0	27.9
TW-2	234.9	372.2	353.2	25.1
TW-3	235.1	366.7	347.8	25.5

<sup>a</sup>  $T_0$ : the temperature at which the sample begins to decompose;  $T_f$ : the temperature at which maximum weight loss is reached during decomposition;  $T_{\max}$ : the temperature at which the decomposition rate is at its maximum.

TW, while no significant change in the Tf of BW is observed, whereas the Tf of TW decreases a lot. Meanwhile, compared with NW and BW, the carbon retention rate of TW is significantly higher (from 18.9% to 27.9%), which indicates that TW has a specific flame retardant property.<sup>38</sup>

## 4. Conclusions

In conclusion, we explored the effective methods of different DES solutions to enhance the bending properties of ash wood through comparative experiments, in which the optimal DES formulation was a ternary DES system of lactic acid/ferric chloride/choline chloride with a water content of 10 wt% (molar ratio of 10 : 1 : 1). Treatment of ash wood strips under this formulation was able to achieve an elongation at break of 7.3% and increase the displacement at which breakage occurs in three-point bending to 20 mm, which effectively improved the bending properties of ash wood strips. The use of DES is indeed a more energy-efficient and eco-friendly way of bending wood compared to other chemical methods. It can even be recycled, and its reaction with lignin can bring about a significant color change. Hence, this formula's emergence can significantly increase the flexibility of wood products and broaden the development prospects of wood in various fields, including construction and furniture.

## Conflicts of interest

The authors declare no competing financial interest.

## Acknowledgements

The authors gratefully acknowledgment the financial support from the Peoples' Republic of China. The authors gratefully acknowledge the financial support from the project funded by the National Natural Science Foundation of China (32071687 and 32001382), 14th Five-Year Key R&D Project on Key Technologies for Manufacturing New Materials for Wood Frontiers (2023YFD2201400).

## References

- E. Roszyk, E. Stachowska, J. Majka, P. Mania and M. Broda, Moisture-Dependent Strength Properties of Thermally-Modified *Fraxinus excelsior* Wood in Compression, *Materials*, 2020, **13**, 1–14.
- J. Ratnasingam, H. Ab Latib, L. Choon Liat and S. Reza Farrokhpayam, Comparative steam bending characteristics of some planted forest wood species in Malaysia, *BioResources*, 2022, **17**, 4937–4951.
- S. d. O. Araujo, B. R. Vital, B. Oliveira, A. d. C. Oliveira Carneiro, A. Lourenco and H. Pereira, Physical and mechanical properties of heat treated wood from *Aspidosperma populifolium*, *Dipteryx odorata* AND *Mimosa scabrella*, *Maderas: Cienc. Tecnol.*, 2016, **18**, 143–156.
- R. E. Hernández, *Influence of Accessory Substances, Wood Density and Interlocked Grain on the Compressive Properties of Hardwoods*, *Wood Science and Technology*, 2006, vol. 41.
- M. Mubarok, H. Militz, S. Dumarcay, W. Darmawan, Y. S. Hadi and P. Gérardin, Mechanical properties and biological durability in soil contact of chemically modified wood treated in an open or in a closed system using glycerol/maleic anhydride systems, *Wood Mater. Sci. Eng.*, 2021, **17**, 356–365.
- M. L. de Peres, R. de Ávila Delucis, D. A. Gatto and R. Beltrame, Mechanical behavior of wood species softened by microwave heating prior to bending, *Eur. J. Wood Wood Prod.*, 2015, **74**, 143–149.
- C. Alvarez-Vasco, R. S. Ma, M. Quintero, M. Guo, S. Geleynse, K. K. Ramasamy, M. Wolcott and X. Zhang, Unique low-molecular-weight lignin with high purity extracted from wood by deep eutectic solvents (DES): a source of lignin for valorization, *Green Chem.*, 2016, **18**, 5133–5141.
- K. Wang, X. Liu, Y. Tan, W. Zhang, S. Zhang and J. Li, Two-dimensional membrane and three-dimensional bulk aerogel materials via top-down wood nanotechnology for multibehavioral and reusable oil/water separation, *Chem. Eng. J.*, 2019, **371**, 769–780.
- W. H. Wang, M. Y. Chen and Y. Wu, Compressible Cellulose Wood Prepared with Deep Eutectic Solvents and Its Improved Technology, *Polymers*, 2023, **15**, 1593.
- T. Sheng, J. Ou, T. Zhao, X. Yang and Y.-X. Peng, Efficient fixation of CO<sub>2</sub> into cyclic carbonate catalyzed by choline bromide/imidazole derivatives-based deep eutectic solvents, *Mol. Catal.*, 2023, **536**, 112907.
- X. D. Hou, A. L. Li, K. P. Lin, Y. Y. Wang, Z. Y. Kuang and S. L. Cao, Insight into the structure-function relationships of deep eutectic solvents during rice straw pretreatment, *Bioresour. Technol.*, 2018, **249**, 261–267.
- W. Pei, Y. Yusufu, Y. Zhan, X. Wang, J. Gan, L. Zheng, P. Wang, K. Zhang and C. Huang, Biosynthesizing lignin dehydrogenation polymer to fabricate hybrid hydrogel composite with hyaluronic acid for cartilage repair, *Adv. Compos. Hybrid Mater.*, 2023, **6**, 180.
- G. J. Lyu, T. F. Li, X. X. Ji, G. H. Yang, Y. Liu, L. A. Lucia and J. C. Chen, Characterization of Lignin Extracted from Willow by Deep Eutectic Solvent Treatments, *Polymers*, 2018, **10**, 869.
- W. R. Xing, G. C. Xu, J. J. Dong, R. Z. Han and Y. Ni, Novel dihydrogen-bonding deep eutectic solvents: Pretreatment of rice straw for butanol fermentation featuring enzyme recycling and high solvent yield, *Chem. Eng. J.*, 2018, **333**, 712–720.
- Q. Q. Xia, Y. Z. Liu, J. Meng, W. K. Cheng, W. S. Chen, S. X. Liu, Y. X. Liu, J. Li and H. P. Yu, Multiple hydrogen bond coordination in three-constituent deep eutectic solvents enhances lignin fractionation from biomass, *Green Chem.*, 2018, **20**, 2711–2721.
- S. Long, Y. Feng, B. Chen, L. Gan, X. Zeng, M. Long and J. Liu, Deep eutectic solvents promote the formation of ultradispersed ZrO<sub>2</sub> in cellulose-based carbon aerogel for



the transfer hydrogenation of biomass aldehydes, *Mol. Catal.*, 2023, **541**, 113106.

17 R. Ninayan, A. S. Levshakova, E. M. Khairullina, O. S. Vezo, I. I. Tumkin, A. Ostendorf, L. S. Logunov, A. A. Manshina and A. Y. Shishov, Water-induced changes in choline chloride-carboxylic acid deep eutectic solvents properties, *Colloids Surf., A*, 2023, **679**, 132543.

18 C. L. Yiin, A. T. Quitain, S. Yusup, Y. Uemura, M. Sasaki and T. Kida, Sustainable green pretreatment approach to biomass-to-energy conversion using natural hydro-low-transition-temperature mixtures, *Bioresour. Technol.*, 2018, **261**, 361–369.

19 A. Mandal and D. Chakrabarty, Isolation of nanocellulose from waste sugarcane bagasse (SCB) and its characterization, *Carbohydr. Polym.*, 2011, **86**, 1291–1299.

20 B. H. A. Sluiter, R. Ruiz and C. Scarlata, *Determination of Structural Carbohydrates and Lignin*, National Renewable Energy Laboratory, 2012.

21 T. Tanimoto and T. Nakano, Difference in reduction properties between longitudinal dimension and elastic modulus of wood induced with aqueous NaOH treatment: modeling and analysis, *J. Wood Sci.*, 2016, **62**, 12–19.

22 Y. Wu, J. C. Zhou, Q. T. Huang, F. Yang, Y. J. Wang, X. M. Liang and J. Z. Li, Study on the Colorimetry Properties of Transparent Wood Prepared from Six Wood Species, *ACS Omega*, 2020, **5**, 1782–1788.

23 M. Wang, R. N. Li, G. X. Chen, S. H. Zhou, X. Feng, Y. Chen, M. H. He, D. T. Liu, T. Song and H. S. Qi, Highly Stretchable, Transparent, and Conductive Wood Fabricated by *in situ* Photopolymerization with Polymerizable Deep Eutectic Solvents, *ACS Appl. Mater. Interfaces*, 2019, **11**, 14313–14321.

24 X. Wang, Y. Zhang, J. Luo, T. Xu, C. Si, A. J. C. Oscanoa, D. Tang, L. Zhu, P. Wang and C. Huang, Printability of hybridized composite from maleic acid-treated bacterial cellulose with gelatin for bone tissue regeneration, *Adv. Compos. Hybrid Mater.*, 2023, **6**, 134.

25 C. Jia, H. Y. Bian, T. T. Gao, F. Jiang, I. M. Kierzewski, Y. L. Wang, Y. G. Yao, L. H. Chen, Z. Q. Shao, J. Y. Zhu and L. B. Hu, Thermally Stable Cellulose Nanocrystals toward High-Performance 2D and 3D Nanostructures, *ACS Appl. Mater. Interfaces*, 2017, **9**, 28922–28929.

26 M. Zhu, Y. Li, G. Chen, F. Jiang, Z. Yang, X. Luo, Y. Wang, S. D. Lacey, J. Dai, C. Wang, C. Jia, J. Wan, Y. Yao, A. Gong, B. Yang, Z. Yu, S. Das and L. Hu, *Tree-Inspired Design for High-Efficiency Water Extraction*, 2017, vol. 29, p.1704107.

27 A. K. Kumar, B. S. Parikh and M. Pravakar, Natural deep eutectic solvent mediated pretreatment of rice straw: bioanalytical characterization of lignin extract and enzymatic hydrolysis of pretreated biomass residue, *Environ. Sci. Pollut. Res.*, 2016, **23**, 9265–9275.

28 H. M. Lou, H. R. Lai, S. Wu, X. L. Li, D. J. Yang, X. Q. Qiu, J. H. Huang and C. H. Yi, Enhancing enzymatic hydrolysis of crystalline cellulose and lignocellulose by adding long-chain fatty alcohols, *Cellu.*, 2014, **21**, 3361–3369.

29 M. W. Zhu, C. Jia, Y. L. Wang, Z. Q. Fang, J. Q. Dai, L. S. Xu, D. F. Huang, J. Y. Wu, Y. F. Li, J. W. Song, Y. G. Yao, E. Hitz, Y. B. Wang and L. B. Hu, Isotropic Paper Directly from Anisotropic Wood: Top-Down Green Transparent Substrate Toward Biodegradable Electronics, *ACS Appl. Mater. Interfaces*, 2018, **10**, 28566–28571.

30 S. L. Xiao, C. J. Chen, Q. Q. Xia, Y. Liu, Y. Yao, Q. Y. Chen, M. Hartsfield, A. Brozena, K. K. Tu, S. J. Eichhorn, Y. G. Yao, J. G. Li, W. T. Gan, S. Q. Shi, V. W. Yang, M. Lo Ricco, J. Y. Zhu, I. Burgert, A. Luo, T. Li and L. B. Hu, Lightweight, strong, moldable wood *via* cell wall engineering as a sustainable structural material, *Sci.*, 2021, **374**, 465–471.

31 H. Chen, J. Y. Wu, J. J. Shi, W. F. Zhang and H. K. Wang, Effect of alkali treatment on microstructure and thermal stability of parenchyma cell compared with bamboo fiber, *Ind. Crops Prod.*, 2021, **164**, 113380.

32 E. S. Jang and C. W. Kang, Changes in gas permeability and pore structure of wood under heat treating temperature conditions, *J. Wood Sci.*, 2019, **65**, 37.

33 T. Nakano, Mechanism of microfibril contraction and anisotropic dimensional changes for cells in wood treated with aqueous NaOH solution, *Cellu.*, 2010, **17**, 711–719.

34 Y. Ran, D. Lu, J. Jiang, Y. Huang, W. Wang and J. Cao, Deep eutectic solvents-assisted wood densification: A promising strategy for shape-fixation, *Chem. Eng. J.*, 2023, **471**, 144476.

35 Z. Qi, H. Cai, F. Ren, L. Liu, K. Yang and X. Han, In-situ lignin regeneration strategy to improve the interfacial combination, mechanical properties and stabilities of wood-plastic composites, *Compos. Sci. Technol.*, 2024, **246**, 0266–3538.

36 R. J. Lin, A. Li, T. T. Zheng, L. B. Lu and Y. Cao, Hydrophobic and flexible cellulose aerogel as an efficient, green and reusable oil sorbent, *RSC Adv.*, 2015, **5**, 82027–82033.

37 T. Faravelli, A. Frassoldati, G. Migliavacca and E. Ranzi, Detailed kinetic modeling of the thermal degradation of lignins, *Biomass Bioenergy*, 2010, **34**, 290–301.

38 P. Phitsuwan, K. Sakka and K. Ratanakhanokchai, Structural changes and enzymatic response of Napier grass *Pennisetum purpureum* stem induced by alkaline pretreatment, *Bioresour. Technol.*, 2016, **218**, 247–256.

